

# THE $K^+ \rightarrow \pi^+ \nu \bar{\nu}$ DECAY AND NEW PHYSICS SEARCHES AT NA62\*

RICCARDO LOLLINI

for the NA62 Collaboration†

Università degli Studi di Perugia and INFN — Sezione di Perugia, Italy

`riccardo.lollini@pg.infn.it`

(Received August 26, 2020)

The NA62 experiment at CERN was designed to measure the branching ratio of the ultra-rare  $K^+ \rightarrow \pi^+ \nu \bar{\nu}$  decay with a decay-in-flight technique. The Standard Model prediction for this branching ratio is very precise and this process is an ideal candidate for the indirect search of New Physics at high-mass scale. NA62 took physics data from 2016 to 2018: the results of the  $K^+ \rightarrow \pi^+ \nu \bar{\nu}$  analysis in the 2016+2017 data sets are presented. Moreover, the high-intensity setup, the flexibility of its trigger system, and the hermetic coverage of the experiment make NA62 a useful tool for the search of exotic particles in the MeV–GeV range weakly coupled to the Standard Model, such as heavy neutral leptons and dark photons. The status of these analyses will be reviewed, along with other New Physics studies carried out at NA62, such as the search for lepton flavour and lepton number violating  $K^+$  decays.

DOI:10.5506/APhysPolBSupp.14.41

## 1. The $K^+ \rightarrow \pi^+ \nu \bar{\nu}$ decay

The branching ratio of the ultra-rare  $K^+ \rightarrow \pi^+ \nu \bar{\nu}$  decay (hereafter also referred to as  $\pi \nu \nu$ ) provides an extremely interesting test of the Standard Model (SM). This decay is a flavour changing neutral current, proceeding through box and electroweak penguin diagrams. Theoretically, this process is very clean and the main sources of uncertainty on the branching ratio originate from the uncertainties on the CKM matrix elements. The SM prediction for the branching ratio is  $\text{BR}(K^+ \rightarrow \pi^+ \nu \bar{\nu}) = (8.4 \pm 1.0) \times 10^{-11}$  [1], while the branching ratio was measured by the BNL E797/E949 experiments that found a value of  $\text{BR}(K^+ \rightarrow \pi^+ \nu \bar{\nu}) = (17.3_{-10.5}^{+11.5}) \times 10^{-11}$ , using stopped kaons [2].

\* Presented at *Excited QCD 2020*, Krynica Zdrój, Poland, February 2–8, 2020.

† The list of NA62 Collaboration members can be found at the end of the article.

The branching ratios of  $K^+ \rightarrow \pi^+ \nu \bar{\nu}$  and  $K_L \rightarrow \pi^0 \nu \bar{\nu}$  define the CKM unitarity triangle independently of the measurements on the  $B$ -meson sector, and a plethora of models beyond the SM (BSM) predict sizeable differences with respect to the SM value [3]. This, together with the accurate theoretical prediction, make  $K^+ \rightarrow \pi^+ \nu \bar{\nu}$  an ideal candidate for the search of New Physics (NP) at high-mass scale.

## 2. The NA62 detector

NA62 is a fixed target experiment located at the North Area of the CERN SPS. The experiment aims at measuring the branching ratio of the  $K^+ \rightarrow \pi^+ \nu \bar{\nu}$  decay with a decay-in-flight technique that allows to have a significant flux of kaons ( $O(10^{13})$ ) over a few years of data taking.

The NA62 detector is schematically depicted in Fig. 1. A 400 GeV/ $c$  proton beam extracted from the SPS impinges on a beryllium target, producing a 75 GeV/ $c$  positively charged hadron beam, with 6%  $K^+$ . Charged kaons are identified by the KTAG, a Cerenkov differential counter, while their momentum is measured by a silicon pixel beam tracker composed of three stations, the GTK. Inelastic interactions in the last GTK station are vetoed by the CHANTI. The fiducial decay region is a 60 m long vacuum vessel, ending with a magnetic spectrometer, measuring the decay products momentum; the spectrometer is made of four straw chambers with a dipole magnet between the second and the third chamber. The particle identification (PID) relies on a RICH detector that is used to distinguish muons from charged pions, and an electromagnetic calorimeter filled with liquid krypton (LKr) that allows to identify  $\gamma$ s and  $e^+$ s from  $K^+$  decays, followed by the hadronic calorimeters MUV1 and MUV2. Further muon suppression is provided by the MUV3, a fast scintillator array at the downstream end of the detector. The CHOD, a scintillator hodoscope, measures the crossing time of charged particles and produces an L0 trigger signal. Finally, a set of

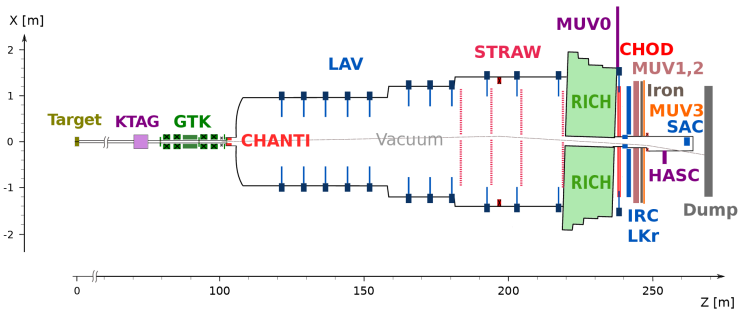


Fig. 1. Schematic top view of the NA62 detector. The trajectory of an undecayed beam particle in vacuum is shown.

several photon veto detectors (LAV, LKr, IRC and SAC) provide hermetical coverage up to 50 mrad. A detailed description of the NA62 apparatus can be found in [4].

NA62 took its first physics run in 2016; in 2017 and 2018, the experiment collected, respectively,  $\sim 10$  and  $\sim 20$  times more data than in 2016, with an overall better collection efficiency.

### 3. The $K^+ \rightarrow \pi^+ \nu \bar{\nu}$ analysis

The results of the  $K^+ \rightarrow \pi^+ \nu \bar{\nu}$  analysis of 2016 data were published in 2019, with the observation of one event in the signal region [5]; in the following, the preliminary results of the analysis of 2017 data (corresponding to  $\sim 2 \times 10^{12}$   $K^+$  decays) will be presented, together with the upper limits on the BR obtained from the combination of 2016 and 2017 data. The signature of  $K^+ \rightarrow \pi^+ \nu \bar{\nu}$  consists in a charged track in the initial state and one in the final state, with undetected energy from the neutrinos. The main variable used for the kinematic selection is the squared missing mass, defined as  $m_{\text{miss}}^2 = (P_K - P_\pi)^2$ , where  $P_K$  and  $P_\pi$  are the 4-momenta of the  $K^+$  and the  $\pi^+$ , respectively. The kaon decays mainly contributing to the background are  $K^+ \rightarrow \mu^+ \nu_\mu$  ( $K_{\mu\nu}$ ),  $K^+ \rightarrow \pi^+ \pi^0$  ( $K_{\pi\pi}$ ),  $K^+ \rightarrow \pi^+ \pi^+ \pi^-$  ( $K_{\pi\pi\pi}$ ),  $K^+ \rightarrow \pi^+ \pi^- e^+ \nu_e$  ( $K_{e4}$ ), and  $K^+ \rightarrow l^+ \pi^0 \nu_l$  ( $K_{l3}$ ). Since the  $m_{\text{miss}}^2$  distribution of  $K_{\pi\pi}$  decays form a sharp peak around the  $\pi^0$  mass, right in the middle of the signal distribution, two separate signal regions are defined: Region 1 (R1) between the  $K_{\mu\nu}$  and  $K_{\pi\pi}$  contributions, and Region 2 (R2) between the  $K_{\pi\pi}$  and  $K_{\pi\pi\pi}$  contributions.  $K_{\mu\pi}$  and  $K_{\pi\pi}$  events can enter anyway these regions through the non-Gaussian resolutions and radiative tails, and  $K_{\pi\pi\pi}$  could enter R2 through the non-Gaussian resolution. Another important contribution to the background comes from the so-called *upstream background*, *i.e.* early kaon decays or beam particle interactions happening upstream the fiducial decay volume and reaching the fiducial region.

A single-track topology is required, asking for a STRAW track matched to a signal in the CHOD and in the RICH. The downstream track is then matched to the upstream track, identified as a kaon in the KTAG and whose momentum is measured by the GTK; the decay vertex is required to be in the fiducial volume. The PID relies on the RICH and on the calorimetric energy reconstructed in the LKr, MUV1 and MUV2. Further suppression against  $K_{\pi\pi}$  is achieved rejecting events with extra-activity in time coincidence with the  $\pi^+$  in LAV, LKr, IRC and SAC. The selection is restricted to  $\pi^+$  with a momentum range of (15, 35) GeV/c in order to have at least 40 GeV/c of extra-energy to veto background events. Combining the

information from the CHOD and the STRAW, events with photon interacting with the material upstream the calorimeter are rejected. Furthermore, events with activity in the CHANTI or extra hits in the GTK are rejected.

In order to evaluate the background from  $K_{\mu\nu}$ ,  $K_{\pi\pi}$  and  $K_{\pi\pi\pi}$ , the kinematic tails of the distributions are extrapolated into the signal regions. In particular, the shape of the tails inside the signal region is modelled using data collected with the control trigger; subsequently, the tails are applied to the number of events surviving the  $\pi\nu\nu$  selection in each background region. Several control regions, adjacent to the signal regions, are defined in order to validate the background evaluation procedure. The evaluation of the background from other  $K^+$  decays relies on the Monte Carlo simulations, validated with the analysis of background-enriched data samples. The contribution of upstream background events in the signal region is computed using the probability of matching a  $\pi^+$  to a pile-up beam particle and the number of events surviving the  $\pi\nu\nu$  selection with inverted  $K^+ - \pi^+$  matching criteria. The single event sensitivity (SES), which by definition is  $\text{BR}_{\pi\nu\nu}/N_{\pi\nu\nu}$ , is measured to be  $\text{SES} = (0.389 \pm 0.021) \times 10^{-10}$ , corresponding to  $N_{\pi\nu\nu} = 2.16 \pm 0.12 \pm 0.26_{\text{ext}}$  expected signal events in R1 and R2. The number of expected background events in the signal region is reported in Table I, together with the number of signal events expected assuming the SM.

TABLE I

Expectation for signal and the background events in the signal region.

Process	Expected events
$K^+ \rightarrow \pi^+ \nu \bar{\nu}$ (SM)	$2.16 \pm 0.12 \pm 0.26_{\text{ext}}$
$K^+ \rightarrow \pi^+ \pi^0(\gamma)$ IB	$0.29 \pm 0.03_{\text{stat}} \pm 0.03_{\text{syst}}$
$K^+ \rightarrow \mu^+ \nu_\mu(\gamma)$ IB	$0.11 \pm 0.02_{\text{stat}} \pm 0.03_{\text{syst}}$
$K^+ \rightarrow \mu^+ \nu_\mu(\mu^+ \rightarrow e^+ \text{ decay})$	$0.04 \pm 0.02_{\text{syst}}$
$K^+ \rightarrow \pi^+ \pi^- e^+ \nu_e$	$0.12 \pm 0.05_{\text{stat}} \pm 0.03_{\text{syst}}$
$K^+ \rightarrow \pi^+ \pi^+ \pi^-$	$0.02 \pm 0.02_{\text{syst}}$
$K^+ \rightarrow \pi^+ \gamma \gamma$	$0.005 \pm 0.005_{\text{syst}}$
$K^+ \rightarrow l^+ \pi^0 \nu_l$	negligible
Upstream background	$0.9 \pm 0.2_{\text{stat}} \pm 0.2_{\text{syst}}$
Total background	$1.5 \pm 0.2_{\text{stat}} \pm 0.2_{\text{syst}}$

#### 4. Results of the $K^+ \rightarrow \pi^+ \nu \bar{\nu}$ analysis

After un-blinding the signal regions, 2 events were found (Fig. 2), in agreement with the number of signal and background events expected. Once combined with the event observed in 2016 data, the three events lead to an

overall  $\text{SES} = (0.346 \pm 0.017) \times 10^{-10}$  and  $1.65 \pm 0.31$  background events expected. Upper limits on the branching ratio of  $K^+ \rightarrow \pi^+ \nu \bar{\nu}$  can be computed using the CLs method [6]. In particular, a simple counting approach gives as a preliminary result  $\text{BR}(K^+ \rightarrow \pi^+ \nu \bar{\nu}) < 1.85 \times 10^{-10}$  at 90% C.L. This results indirectly lead to an upper limit on the branching ratio of  $K_L \rightarrow \pi^0 \nu \bar{\nu}$  thanks to the Grossman–Nir limit [7]:  $\text{BR}(K_L \rightarrow \pi^0 \nu \bar{\nu}) < 8.14 \times 10^{-10}$  at 90% C.L.

Due to the extremely good  $\pi^0$  rejection needed to suppress the  $K\pi\pi$  background, NA62 can perform the search for the decay  $\pi^0 \rightarrow \text{invisible}$  as a direct byproduct of the  $\pi\nu\nu$  analysis. In particular, using roughly one third of the 2017  $\pi\nu\nu$  data, this search leads to an upper limit  $\text{BR}(\pi^0 \rightarrow \text{invisible}) < 4.4 \times 10^{-9}$  at 90% C.L., which is a significant improvement of the state of the art.

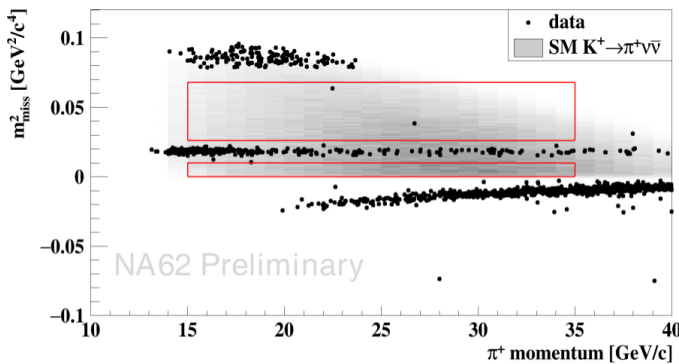


Fig. 2. (Colour on-line)  $m^2_{\text{miss}}$  versus  $p_\pi$  distribution of events surviving the  $K^+ \rightarrow \pi^+ \nu \bar{\nu}$  selection. The signal regions 1 and 2 are defined by grey/red boxes, the grey area corresponds to the distribution of simulated signal events.

## 5. Exotic searches

Thanks to its hermetic, high-efficiency photon veto, redundant PID, and a high-intensity hadron beam, NA62 is particularly suitable for the search of NP in the MeV–GeV range, feebly coupled to SM particles, via detection of long-lived particles produced in the target or in the beam collimators when used as a beam dump, or via detection of NP in kaon decays.

Lepton number and lepton flavour violations (LNV/LFV) in kaon decays are predicted in NP models via Majorana neutrinos [8, 9]. In particular, NA62 can search for  $K^+ \rightarrow \pi^- e^+ e^-$  and  $K^+ \rightarrow \pi^+ \mu^+ \mu^-$ . The 90% C.L. upper limits resulting from these analyses are  $\text{BR}(K^+ \rightarrow \pi^- e^+ e^-) < 2.2 \times 10^{-10}$  and  $\text{BR}(K^+ \rightarrow \pi^+ \mu^+ \mu^-) < 4.2 \times 10^{-11}$  [10]. These results are based on a subset of 2017 data, three times more data are still to be analysed in

the full data set (2016–2018); nevertheless, these upper limits improve the state of the art by a factor 3 (for the electron channel) and 2 (for the muon channel).

NA62 can also search for heavy neutral leptons (HNL) [11] of a few hundreds MeV produced in kaon decays, such as  $K^+ \rightarrow e^+ N$  and  $K^+ \rightarrow \mu^+ N$  [12]. A mass scan was performed in the range of 141–462 (220–383) MeV/ $c^2$  in the  $e^+$  ( $\mu^+$ ) channel. The preliminary results of the analysis on 2016+2017 data have recently been presented in [13]: no excess was found and the new upper limits on the mixing parameters improved by more than 2 orders of magnitude with respect to previous results (Fig. 3, left). Another factor 2 of improvement is expected when the full data set will be analysed.

Searches for a dark photon (DP) [14] not decaying into SM particles can be performed at NA62. Figure 3, right shows the 90% C.L. exclusion limits in the mass of the DP *versus* coupling plane ( $M_{A'}$ ,  $\epsilon^2$ ) for the search of an invisible DP [15]. The search is performed selecting  $K^+ \rightarrow \pi^+ \pi^0$  decays where  $\pi^0 \rightarrow \gamma A'$  and  $A' \rightarrow$  invisible. This result relies on the analysis of a subsample of 2016 data, corresponding to 1% of the complete data set (2016–2018). As a byproduct of this analysis, with just a few modifications, it is possible to search for the  $\pi^0 \rightarrow \gamma \nu \bar{\nu}$  decay. The SM expectation for the branching ratio of this process is of the order of  $10^{-18}$ : NA62 put an upper limit of  $\text{BR}(\pi^0 \rightarrow \gamma \nu \bar{\nu}) < 1.9 \times 10^{-7}$  at 90% C.L., improving by more than 3 order of magnitudes with respect to earlier searches.

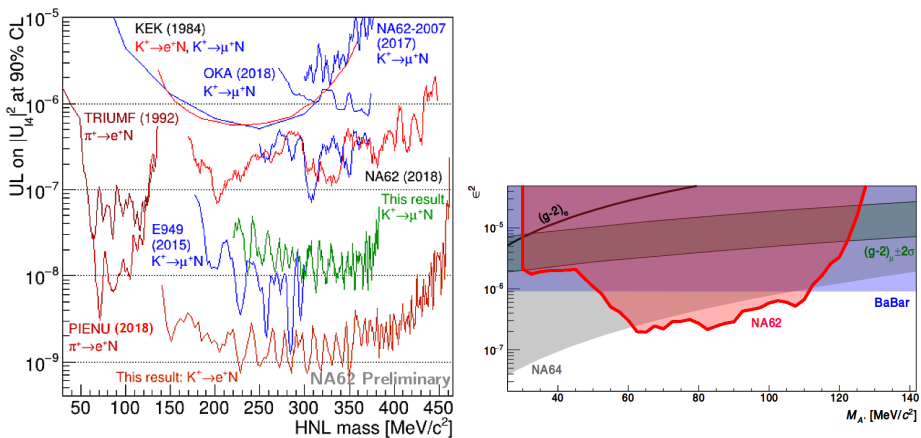


Fig. 3. (Colour on-line) Left: preliminary upper limits at 90% C.L. on  $|U_{l4}|^2$  for each HNL mass compared to the results obtained from earlier searches. Right: upper limits at 90% C.L. in the coupling *versus*  $M_{A'}$  for the NA62 search of  $\pi^0 \rightarrow \gamma A'$  with  $A' \rightarrow$  invisible (grey/red area), together with the limits obtained by NA64 and BaBar.

Finally, NA62 can perform several direct searches of exotic particles visible decays produced dumping the beam after the target (Fig. 4), such as axion-like particles (ALPs) decaying into two photons, DPs decaying into two charged leptons, dark scalars decaying into a pair of muons, and HNLs decaying into a pion and a charged lepton. NA62 already took some beam dump data to study the background for future beam dump data taking: in particular, beam dump runs are foreseen after the long shutdown 2 to collect  $O(10^{18})$  protons on target. More details can be found in [16].

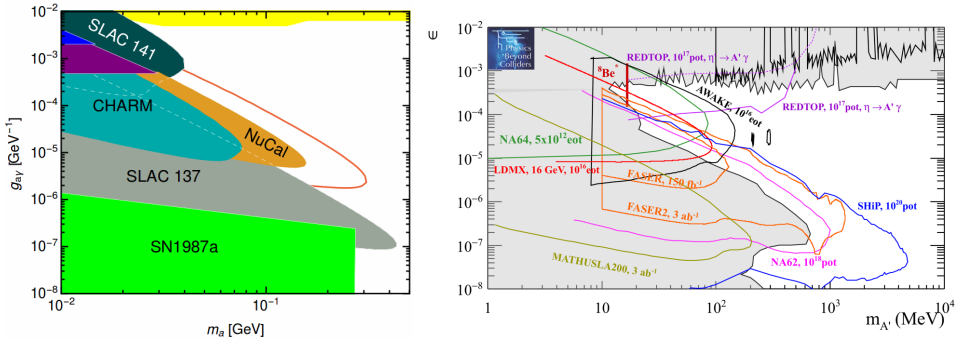


Fig. 4. (Colour on-line) NA62 expected 90% C.L. exclusion limits for  $10^{18}$  protons on target in the coupling *versus* mass plane for ALPs decaying into two photons (left, orange solid line) and for the visible decay of a DP (right, magenta solid line).

## REFERENCES

- [1] A.J. Buras *et al.*, *J. High Energy Phys.* **1511**, 33 (2015).
- [2] E949 Collaboration, *Phys. Rev. D* **79**, 092004 (2009).
- [3] M. Blanke *et al.*, *J. High Energy Phys.* **0903**, 108 (2009); A.J. Buras *et al.*, *J. High Energy Phys.* **1511**, 166 (2015); T. Blažek, P. Maták, *Int. J. Mod. Phys. A* **29**, 1450162 (2014); G. Isidori *et al.*, *J. High Energy Phys.* **0608**, 064 (2006); M. Blanke *et al.*, *Eur. Phys. J. C* **76**, 182 (2016); M. Bordone *et al.*, *Eur. Phys. J. C* **77**, 618 (2017).
- [4] NA62 Collaboration, *JINST* **12**, P05025 (2017).
- [5] NA62 Collaboration, *Phys. Lett. B* **791**, 156 (2019).
- [6] A.L. Read, *J. Phys. G: Nucl. Part. Phys.* **28**, 2693 (2002).
- [7] Y. Grossman, Y. Nir, *Phys. Lett. B* **398**, 163 (1997).
- [8] A. Atre *et al.*, *J. High Energy Phys.* **0905**, 030 (2009).
- [9] L.S. Littenberg, R. Shrock, *Phys. Lett. B* **491**, 285 (2000).
- [10] NA62 Collaboration, *Phys. Lett. B* **797**, 134794 (2019).
- [11] T. Asaka, M. Shaposhnikov, *Phys. Lett. B* **620**, 17 (2005).
- [12] NA62 Collaboration, *Phys. Lett. B* **778**, 137 (2018).

- [13] E. Goudzovski,  
<https://indico.cern.ch/event/769729/contributions/3511127/>,  
presentation at KAON 2019.
- [14] B. Holdom, *Phys. Lett. B* **166**, 196 (1986).
- [15] NA62 Collaboration, *J. High Energy Phys.* **1905**, 182 (2019).
- [16] J. Beacham *et al.*, *J. Phys. G: Nucl. Part. Phys.* **47**, 010501 (2020).

List of NA62 Collaboration members:

R. Aliberti, F. Ambrosino, R. Ammendola, B. Angelucci, A. Antonelli,  
G. Anzivino, R. Arcidiacono, T. Bache, A. Baeva, D. Baigarashev, M. Barbanera,  
J. Bernhard, A. Biagioni, L. Bician, C. Biino, A. Bizzeti, T. Blazek,  
B. Bloch-Devaux, V. Bonaiuto, M. Boretto, M. Bragadireanu, D. Britton,  
F. Brizioli, M.B. Brunetti, D. Bryman, F. Bucci, T. Capussela, J. Carmignani,  
A. Ceccucci, P. Cenci, V. Cerny, C. Cerri, B. Checcucci, A. Conovaloff,  
P. Cooper, E. Cortina Gil, M. Corvino, F. Costantini, A. Cotta Ramusino,  
D. Coward, G. D'Agostini, J. Dainton, P. Dalpiaz, H. Danielsson, N. De Simone,  
D. Di Filippo, L. Di Lella, N. Doble, B. Dobrich, F. Duval, V. Duk,  
D. Emelyanov, J. Engelfried, T. Enik, N. Estrada-Tristan, V. Falaleev,  
R. Fantechi, V. Fascianelli, L. Federici, S. Fedotov, A. Filippi, M. Fiorini, J. Fry,  
J. Fu, A. Fucci, L. Fulton, E. Gamberini, L. Gatignon, G. Georgiev, S. Ghinescu,  
A. Gianoli, M. Giorgi, S. Giudici, F. Gonnella, E. Goudzovski, C. Graham,  
R. Guida, E. Gushchin, F. Hahn, H. Heath, E.B. Holzer, T. Husek, O. Hutanu,  
D. Hutchcroft, L. Iacobuzio, E. Iacopini, E. Imbergamo, B. Jenninger, J. Jerhot,  
R.W. Jones, K. Kampf, V. Kekelidze, S. Kholodenko, G. Khorauli,  
A. Khotyantsev, A. Kleimenova, A. Korotkova, M. Koval, V. Kozhuharov,  
Z. Kucerova, Y. Kudenko, J. Kunze, V. Kurochka, V. Kurshetsov, G. Lanfranchi,  
G. Lamanna, E. Lari, G. Latino, P. Laycock, C. Lazzeroni, M. Lenti, G. Lehmann  
Miotto, E. Leonardi, P. Lichard, L. Litov, R. Lollini, D. Lomidze, A. Lonardo,  
P. Lubrano, M. Lupi, N. Lurkin, D. Madigozhin, I. Mannelli, G. Mannocchi,  
A. Mapelli, F. Marchetto, R. Marchevski, S. Martellotti, P. Massarotti,  
K. Massri, E. Maurice, M. Medvedeva, A. Mefodev, E. Menichetti, E. Migliore,  
E. Minucci, M. Mirra, M. Misheva, N. Molokanova, M. Moulson, S. Movchan,  
M. Napolitano, I. Neri, F. Newson, A. Norton, M. Noy, T. Numao, V. Obraztsov,  
A. Ostankov, S. Padolski, R. Page, V. Palladino, A. Parenti, C. Parkinson,  
E. Pedreschi, M. Pepe, M. Perrin-Terrin, L. Peruzzo, P. Petrov, F. Petrucci,  
R. Piandani, M. Piccini, J. Pinzino, I. Polenkevich, L. Pontisso,  
Yu. Potrebenikov, D. Protopopescu, M. Raggi, A. Romano, P. Rubin,  
G. Ruggiero, V. Ryjov, A. Salamon, C. Santoni, G. Saracino, F. Sargeni,  
S. Schuchmann, V. Semenov, A. Sergi, A. Shaikhiev, S. Shkarovskiy, D. Soldi,  
V. Sugonyaev, M. Sozzi, T. Spadaro, F. Spinella, A. Sturgess, J. Swallow,  
S. Trilov, P. Valente, B. Velghe, S. Venditti, P. Vicini, R. Volpe, M. Vormstein,  
H. Wahl, R. Wanke, B. Wrona, O. Yushchenko, M. Zamkovsky, A. Zinchenko.